JETIR.ORG ISSN: 2349-5162 | ESTD Year : 2014 | Monthly Issue
JOURNAL OF EMERGING TECHNOLOGIES AND INNOVATIVE RESEARCH (JETIR)
An International Scholarly Open Access, Peer-reviewed, Refereed Journal

SAW (Designing Surface Acoustic Wave) Gas Sensor Using Dissimilar MEMS Piezoelectrical Materials based on COMSOL - A Comparative Study

[a] Dr. T. S. Jayanthi, [a*] Mr. S. S. Saravanakumar, [b] Mrs. S. Nagadeepa, [c] Dr. Subbiah Rammohan Chitra

[a] Head and Associate Professor, Department of Physics, Vivekananda College, Agasteeswaram, (Affiliated to Manonmaniam Sundaranar University, Tirunelveli), Tamilnadu, India.

[a*]Guest Lecturer, PG and Research Department of Physics, Sethupathy Government Arts College, Ramanathapuram-623502, Tamilnadu, India.

[b] Assiatant Professor, Department of Physics, Sethu Institute of Technology, Kariapatti-626115, Tamilnadu, India.

[c] Head and Associate Professor, Department of Physics, P K N Arts and Science College, Thirumangalam, Madurai, Tamilnadu, India.

[a, a*] Corresponding Authors, [b] Co corresponding Author

Abstract

A surface acoustic wave (SAW) gas sensor allows propagation of the wave through its surface piezoelectric materials. SAW devices are now frequently utilized. In a variety of fields due to their benefits characteristics such as a simple design, low cost, and superb performance, they may also be used in challenging environmental circumstances. Miniaturized Micro-Electro-Mechanical Systems, MEMS-based miniaturized gas sensors have several advantages such as low power, small size, and potential CMOS compatibility. A metal oxide semiconductor is a sensing technology that has a complex interaction with some types of gases such as changing the conductivity while adsorbing gas, giving two independent outputs, mass and resistance change of the material. The object of this work is to design a mass-sensitive transducer that can be integrated with the metal oxide semiconductor. An examination of the SAW gas sensor's materials, architecture design, and analysis of the SAW gas sensor are proposed in this paper. SAW devices were fabricated in commercial MEMS processes using piezoelectrical material such as Zinc oxide (ZnO), Tin Oxide (SnO_2), and Barium titanate ($BaTiO_3$) in form of polycrystalline material. This paper represents a comparative study of a SAW gas sensor with two different designs of interdigitated transducers (IDT) using different piezoelectric materials as a substrate with a sensing layer based on COMSOL Multiphysics 5.5 software to maximize its output. The first design has the shape rectangular (IDT) while the second design has the shape of an ellipse. The designed and the suggested Gas sensor architectures were modeled. The displacement of the surface and electric potential at various eigen frequencies at constant temperature

293K were investigated and contrasted with each other. In the case of gas sensor architectures, the layout which consists of elliptical IDTs offers better behavior as obtained from the material study. Barium titanate has a higher SAW velocity than other materials is 5700 m/s and high sensitivity which reaches 43 for rectangular design, and the elliptical design the sensitivity reaches 49. Regarding power consumption Barium titanate also has lower values for the rectangular and elliptical designs which are 35 mW and 30 mW respectively.

Keywords:

ZnO, SnO_2, $BaTiO_3$, SAW, IDTS, MEMS, COMSOL.

Introduction

Among the various sensors of interest, gas sensing has emerged as one of the most active research topics for applications such as industrial production such as CO_2 sensing for food storage, home security such as CO, volatile organic compounds (VOCs) detection, medical applications such as diabetes diagnosis, and environmental air quality monitoring such as CO_2 monitoring [1-2]. Gas sensors were used to convert the target gas volume into a proportional electrical signal. Sensors, in general, detect physical variations in sensing materials such as conductivity, capacitance, and mechanical deformation caused by loading mass [3].

Furthermore, these devices are accessible in a wide range of electronic components, including actuators, filters, oscillators, and sensors [4-5]. An interdigitated transducer (IDT) is the primary element of the SAW gas sensor and a piezoelectric substrate that has a thin film put on top of it. The interdigitated transducer's electrodes contain comb-like shapes; Impulse signals are converted to acoustic waves by the input IDT, and the process is then reversed by the output IDT SAW systems are currently extensively employed in several disciplines due to their benefits such as construction that is basic, minimal in cost, and good in performance The SAW gas sensor was essentially made out of a piezoelectric platform overlaid with a thin film on top, as well as an IDT at the upper. The IDT's electrodes have comb-like shapes; the I/P IDT was employed to transform impulse signals into acoustic waves, and the O/P IDT was utilized to reverse the process [6]. Inversion of polarity generates an alternating electric field, which creates compressive strain regions via the inverse piezoelectric effect. At that point, a mechanical wave is produced, and it is called the surface acoustic wave [7].

By using the piezoelectric effect, the acoustic wave was processed by converting it back to an electrical signal and sending it. The input and output signals may have different amplitudes, frequencies, and phases. According to the quantity of IDTs and the propagation area, SAW sensors are built in two configurations [8]. In this study, three different materials of substrate layer have been applied, which are ZnO, SnO_2, and $BaTiO_3$. ZnO is a multifunctional material that has applications such as varistors, gas sensors, SAW devices, transparent electrodes, catalysts, and so on. ZnO applications are due to their unique chemical, surface, and microstructural properties [9]. The sensitivity and response time of ZnO-based sensors is strongly influenced by the material's porosity. The polycrystalline zinc oxide material's grain size also has an impact on its gas-sensing properties. It has been experimentally demonstrated that the gas sensitivity of ZnO sensors decreases as the mean grain size increases [10-11]. Because of its high piezoelectric coupling, ZnO is a versatile material for various commercial applications such as piezoelectric devices, and SAW devices [12]. SnO_2 gas sensors are commonly employed to identify combustible

gases in oxygen-rich environments. Adsorbed oxygen species remove electron density from the SnO_2 surface, increasing its electrical resistance. The operating temperature of SnO_2 gas sensors is critical information in studies of their response mechanism [13]. $BaTiO_3$ is a material used for piezoelectric. Because polycrystalline $BaTiO_3$ has a positive temperature coefficient, it can be used in thermistors and self-regulating electric heating systems [14]. This results in composites with a negative bulk modulus (Young's modulus) for barium titanates, which means when a force is thrust to the elements, movement happens in the opposite direction, hardening the mixture even more [15]. Surface acoustic wave gas sensors are used in a variety of applications. Table 1 gives an overview of several applications, including a sensor for volatile gases, a toxic gas sensor, and a wireless antenna resonator [16]. They were all intended to be gas sensors. The eigen frequencies change or shift as various natural gases are detected by the sensor device [17]. As various piezoelectric materials were used as a substrate such as Barium Sodium Niobate, Lithium Niobate, and Quartz, Lithium Niobate was the most popular material used. Sensors are operating with different ranges of varying multiple software used to simulate senor design at different ranges of frequencies such as COMSOL Multiphysics 5.5, MATLAB, and others used the most popular software used is COMSOL [18-19].

Table 1 Sensors are designed for various operating frequencies ranges [16]

Applications	Material	Operation frequency
Sensor for volatile gases	Barium Sodium Niobate	281.589 Hz
Sensor for volatile gases	Lithium Niobate	1.121 GHz
Toxic gas sensor	Lithium Niobate	25.20 MHz
Wireless sensor	Quartz	433.9 MHz
Gas sensor	Lithium Niobate	8.554 GHz
Volatile gas sensor	Lithium Niobate	841 MHz
Gas sensor	Lithium Niobate	1.121 GHz

Sensor and spacer layer influence on SAW velocity was investigated [20]. This work simulates the surface acoustic wave propagation in the commonly utilized $ZnO/Si_3N_4/LiNbO_3$ and $ZnO/SiO_2/LiNbO_3$ layered structures using COMSOL 3.4 and 3.5. It is explored the influence of sensing and spacer layer thickness and composition. SAW sensors may be designed using the simulation findings; The Si_3N_4 spacers have thicknesses of 100nm, 200nm, and 300nm. The ZnO sensor layer has a thickness ranging from 100nm to 1000nm. This research clearly illustrated that when the sensing layer thickness grows, the velocity of a surface acoustic wave reduces significantly and that the resultant velocity is dictated by the eigen frequency corresponding to a surface acoustic wave. The design modeling and evaluation of surface acoustic wave gas sensors based on nanostructures were examined [21]. A multilayer layer structure composed of ZnO (the top layer) and lithium niobate was investigated. A variety of multilayer structures have been described, but $ZnO\text{-}LinbO_3$ is feasible to optimize SAW sensors by considering several intermediate materials with varied dimensions. It was discovered that adjusting the depth of the sensor layer and the

electrode alignment can improve performance. Aside from the frequency change, the overall movement will be enhanced. As a result, SAW-based gas sensors may offer improved sensitivity.

The sensor exhibits linear behavior and a full-scale resolution of 1%. The surface acoustic wave propagation characteristics of ZnO/IDT/128° YX $LiNbO_3$ was discussed in [22]. The Finite Element Method was utilized to do the numerical study using the COMSOL Multiphysics 4.3 platform (FEM). AutoCAD was used to build the IDT pattern. Then put on a color-changing photomask. The samples had a zinc oxide layer deposited on them using RF magnetron sputtering. This led to the investigation of the SAW device's frequency response and coupling coefficient (K_2) in ZnO/IDT/128° YX $LiNbO_3$ with variable ZnO layer thickness. The numerical findings show that in a 1.5 mm thick ZnO sheet, the structure's K_2 has been maximized at 11.7%.

A surface acoustic wave device for sensor application was demonstrated in [23] this case, they employed two different kinds of SAW structures: A delay line, a two-port device with two sets of IDTs, was another name for it. The input IDT, also referred to as the first set of IDTs, smears the signal to create the surface wave and a resonator, a single-port device. To get the best results, you should use a reputable company. SAW delayed line sensor FEM simulation using a simpler model was investigated in [24].

In this study, a two-dimensional finite FEM simulation of a SAW model of a delay line is designed using COMSOL Multiphysics (commercial FEM software). They use the COMSOL Multiphysics direct solver SPOOLES with a time interval of 0.1 ns for 12 ns for an input sine wave with a frequency of 100 MHz and a peak-to-peak (Vin) voltage of 1 V to investigate the spreading of SAW waves through the delay line, as well as the transient evaluation of the SAW delayed line. The main aspects of this paper can be listed as follows: section one presented the introduction about SAW gas sensors and previous work. Section two introduced the component of the SAW gas sensor and section three discussed our methodology which illustrates the material used in different designs for the SAW gas sensor, the design of the SAW gas sensor based on rectangular IDTs, and the design of the SAW gas sensor based on elliptical IDTs. In the next section, the result and discussion presented. The last section is a conclusion.

Components of the SAW gas sensor

Surface Acoustic Wave Devices

A SAW is an acoustic wave that moves elliptically over the shallow surface of a solid and is composed of two separate mechanical waves, compression and shear waves Particle displacements decrease as the depth of the substrate surface increases. As a result of this, the wave's energy is concentrated on the surface and attenuates exponentially away from the surface making it ideal for sensor applications [25].

Different piezoelectric materials were employed to the measurement of physical quantities, such as strain, pressure, and temperature [26]. SAW devices can detect various gases (such as NH_3, H_2, SO_2, NO_2, H_2S, and humidity) [27]. A SAW sensor can be configured in two ways: single port (single IDT) or two ports (double IDTs). The general structure of a two-port SAW delay line type sensor is shown in Figure 1. It is made up of a series of Interdigital Transducers (IDTs) that were fabricated on both ends of a piezoelectric substrate to convert mechanical energy and electric signal [28].

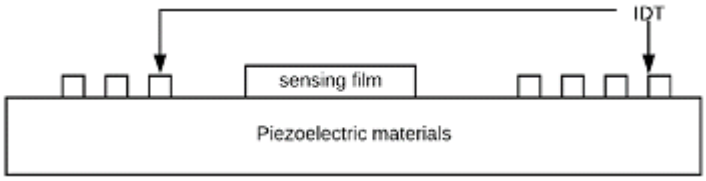

Figure 1 One kind of SAW gas sensor structure [28]

The input IDT turns the excitation electric signal into a SAW utilizing the piezoelectric action. The acoustic wave travels through the delay line region to the output IDT, which converts the mechanical wave back into an electrical signal [29-30]. A SAW device was distinguished by features such as miniature, cheap priced, and fabrication in batches. This is due to its simple structure and use of singlecrystal materials in manufacturing. The materials are readily available, and the fabrication process is well-developed [31-32].

Sensing Schemes

SAW sensors operate based on changes in wave velocity, loss, and other parameters caused by disturbance factors in the sound wave propagation process [33]. This perturbation theory can explain the variation in SAW velocity caused by any factor that can change the mechanical and electrical SAW propagation characteristics [34]. To demonstrate this, a gas sensor with a mass loading sensing mechanism caused by surface displacement was used. The sensing material is deposited along the propagation path between the two IDTs. After being exposed to a target analyte (such as target gas), the sensor's active sensing material adsorbs the analyte molecules, causing the sensing material's mass to increase and the SAW speed to decrease under the sensing material's region. The relative change in wave speed Δv caused by mass loading was designed [35].

Interdigital Transducers (IDTs)

Interdigital electrodes patterned on the surface of the piezoelectric crystal can be used to excite and detect SAW [36]. In their most common form, IDTs are made up of two identical combs-like metal electrodes that alternate in a periodic pattern. One of the combs is grounded, while the other is linked to the RF signal generator [37-38]. The IDT configuration used in this work is shown in Figure 2. A pair of electrodes (two adjacent IDT fingers) from different combs are treated as one period, with a width equal to (p), and the width of each electrode (finger) and the spacing between two adjacent electrodes are (p/4) [39].

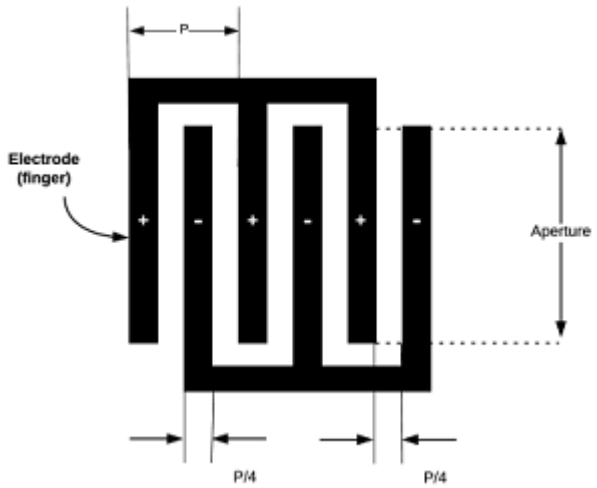

Figure 2 Schematic of Interdigital Transducer (IDT) [39]

When a sinusoidal voltage is applied to the transducer, the wave with the greatest amplitude was produced when the wavelength (λ) matches the transducer periodicity (p). This can be accomplished by activating the IDT at a synchronous frequency [40]. Because of the IDT's symmetry, the mechanical wave propagates equally in both directions from the input IDT. It means that only half of the mechanical wave energy propagates across the delay line in the direction of the output IDT [41]. Changes in the physical properties of the surface of the piezoelectric substrate caused by mass loading under the sensing area cause changes in the SAW propagation characteristics (such as changing the SAW propagation speed and amplitude) when the SAW spreads throughout the substrate's surface. As shown in Figure 3 the Sensing mechanism of a two-port SAW device [42].

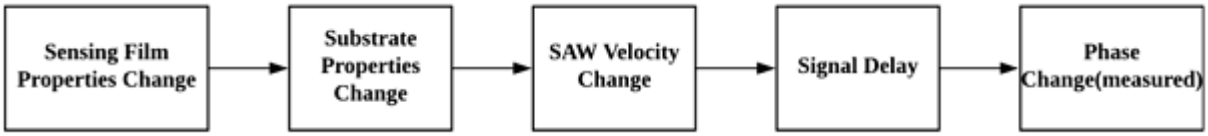

Figure 3 Sensing mechanism of a two-port SAW device [42]

Materials and Methods

This article compares the output of a SAW gas sensor with two different designs of interdigitated transducers (IDT) using different MEMS piezoelectric materials as a substrate and a sensing layer based on COMSOL using Multiphysics 5.5 software. The first design consists of three main parts, substrate material, sensing material, and two IDTs, which is the shape of rectangular. The second design is identical to the first design, but with a different shape of the two IDTs, which is elliptical. One of the key elements affecting a gas sensor's sensitivity is the material's surface acoustic wave velocity. Therefore, the material becomes more sensitive when provided by a higher SAW velocity. Three different piezoelectric materials are employed in the material investigation and the study is carried out for different structures. ZnO, SnO_2, and $BaTiO_3$ are among the components employed in the analysis. These materials' SAW velocities are 2655 m/s, 3750 m/s, and 5700 m/s, respectively. The simulation input is an electromagnetic wave with a specific frequency, surface displacement, and electric potential and is examined as a part of the material analysis process for the output. By using COMSOL Multiphysics 5.5, to acquire precise results, a tiny mesh is produced, and the conditions at the boundary are employed and emulated.

In this paper, three different MEMS piezoelectric materials as a substrate are used to create two different designs. ZnO and SnO_2 in form of polycrystalline are used as the first and second materials to produce the two designs. The properties of ZnO and SnO_2 materials are employed in this study. The tangent coefficient of thermal expansion for ZnO and SnO_2 is 23e-6, the isotropic tangent coefficient of thermal expansion for ZnO and SnO_2 is 0.5e-6 and the coefficient of thermal expansion for both materials is 2.9e-6 at a fixed temperature of 293 K. The third material used is $BaTiO_3$. Polyisobutylene (PIB) is used as a sensing material, which is a gas-impermeable synthetic rubber produced and utilized worldwide to make lubricants, glues, sealants, fuel chemicals, film for clinging, and chewing gum. The IDT is made of aluminum electrodes and is utilized in the conversion of the electromagnetic waves to acoustic waves in addition to the reverse. Aluminum is the most widely used for this purpose [43].

Design of Saw Gas Sensor based on Rectangular IDTs

The suggested SAW gas sensor design is depicted in fig.4. The interdigitated transducers (IDT) utilized in SAW systems are made up of a large number of similar electrodes and the length of the electrode is made 100 times the width to eliminate edge effects. Therefore, modeled geometry is reduced to a periodic unit cell. The cell's height is constructed in such a way that the SAW nearly suffocated at the lowest limit. The substrate is composed of a piezoelectric substance and has a width of 3 μm and a height of 17.5 μm. The conducting electrodes are constructed of aluminum and have a width of 0.75 μm and a height of 0.1 μm. The detecting thin film has a width of 3 μm and a height of 0.5 μm.

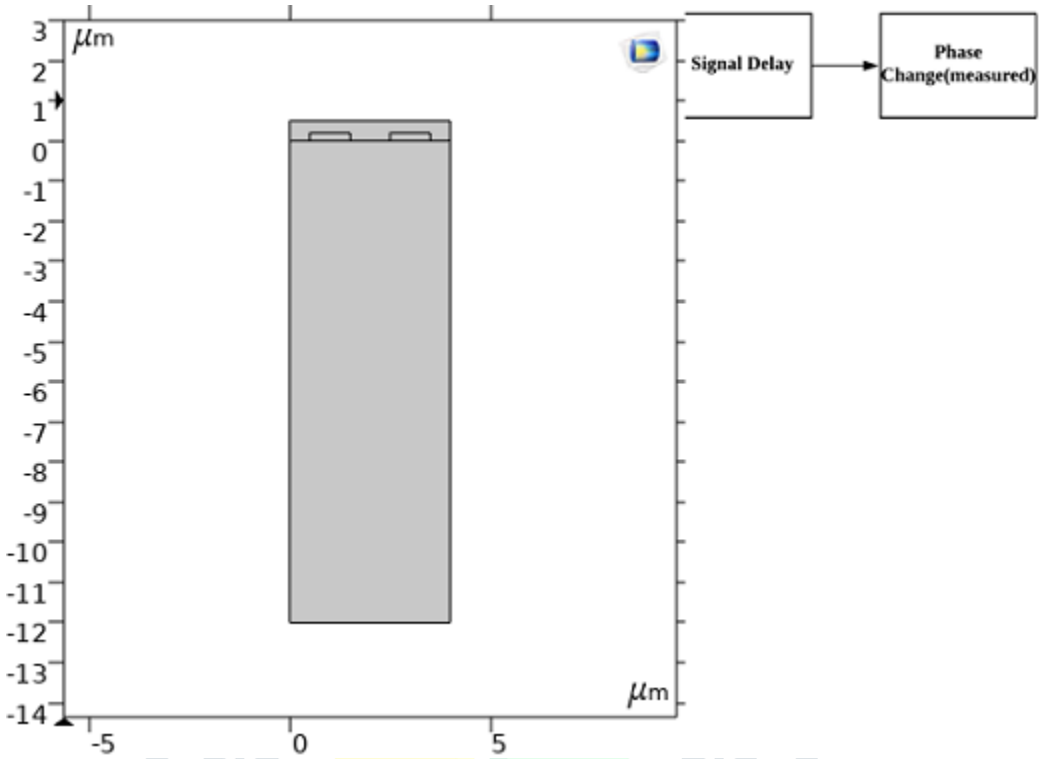

Figure 4 Rectangular structure of the saw gas sensor (in μm)

Design of SAW Gas Sensor based on elliptical IDTs

This design uses an interdigitated transducer structure, shown as two small rectangles, which convert from a rectangular structure to an elliptical one, with an area even more compact than the rectangle.

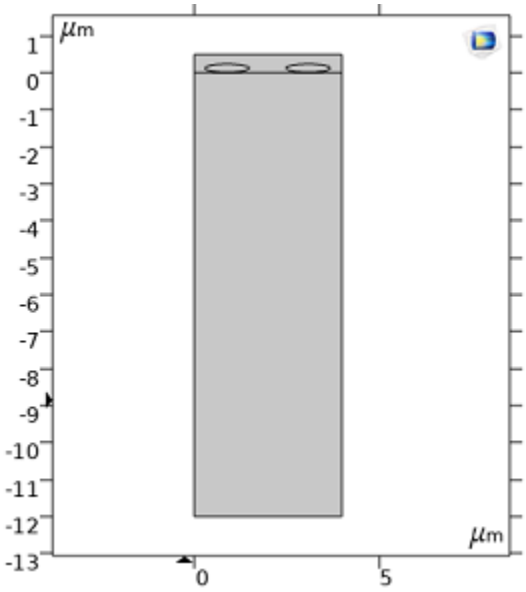

Figure 5 The elliptical structure of the gas sensor (in μm)

The same analysis is then performed and emulated. Figure.5 presents a second designed gas sensor with an elliptical shape with the three studied materials that provide increased sensitivity. The basic substrate structure and SAW gas sensor's thin-film structure are designed in this paper. For greater sensitivity, the interdigitated transducer's rectangular structure is changed to an ellipse. Both interdigitated transducers are designed and simulated using COMSOL Multiphysics 5.5. Height and width both draw attention to the interdigitated transducer's dimensional variance. The width ranged from 0.2 m to 1.2 m. The structures' varying heights do not appear to vary significantly at the output.

Result and Discussion

This section discusses the egin frequency, electric potential, and total surface displacement for the two designs of the SAW gas sensors. Figure 6 demonstrates the resonant SAW phase at a frequency that resonates of 8.1599 E+08 Hz for ZnO and SnO_2 and $BaTiO_3$. Figure 7 represents the electric potential (V) produced by a rectangular-structured SAW sensor. For varied eigenfrequency I/P values, the O/P electric potential changes. The red color zone represents maximal electric potential, and it transitions to blue at lesser values.

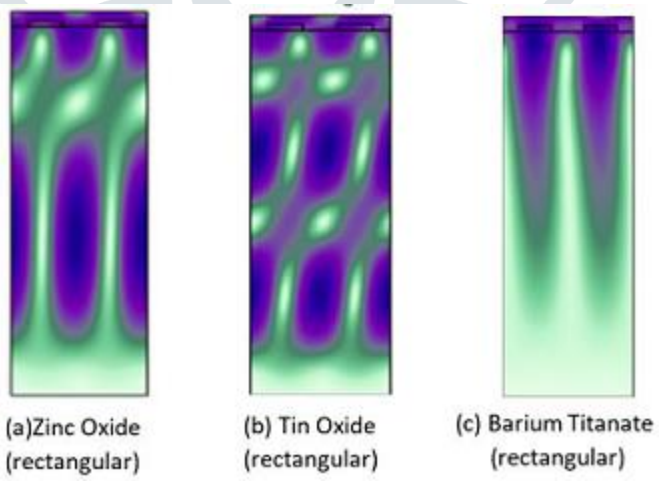

Figure 6 The resonant SAW mode with a resonant frequency of 8.1599 E+08 Hz for ZnO and SnO_2 and $BaTiO_3$

A fine mesh is generated to achieve precise answers, boundary constraints are imposed and simulated using COMSOL Multiphysics 5.5 as shown in Figure 8 the first parameter is a wave of electromagnetic energy with a sppecified frequency, and the simulation output is the wave's surface displacement and electric potential. Figure 9 displays the resonant SAW phase with a frequency of resonance of 8.159E+08 for ZnO and SnO_2 and $BaTiO_3$ for elliptical IDTs.

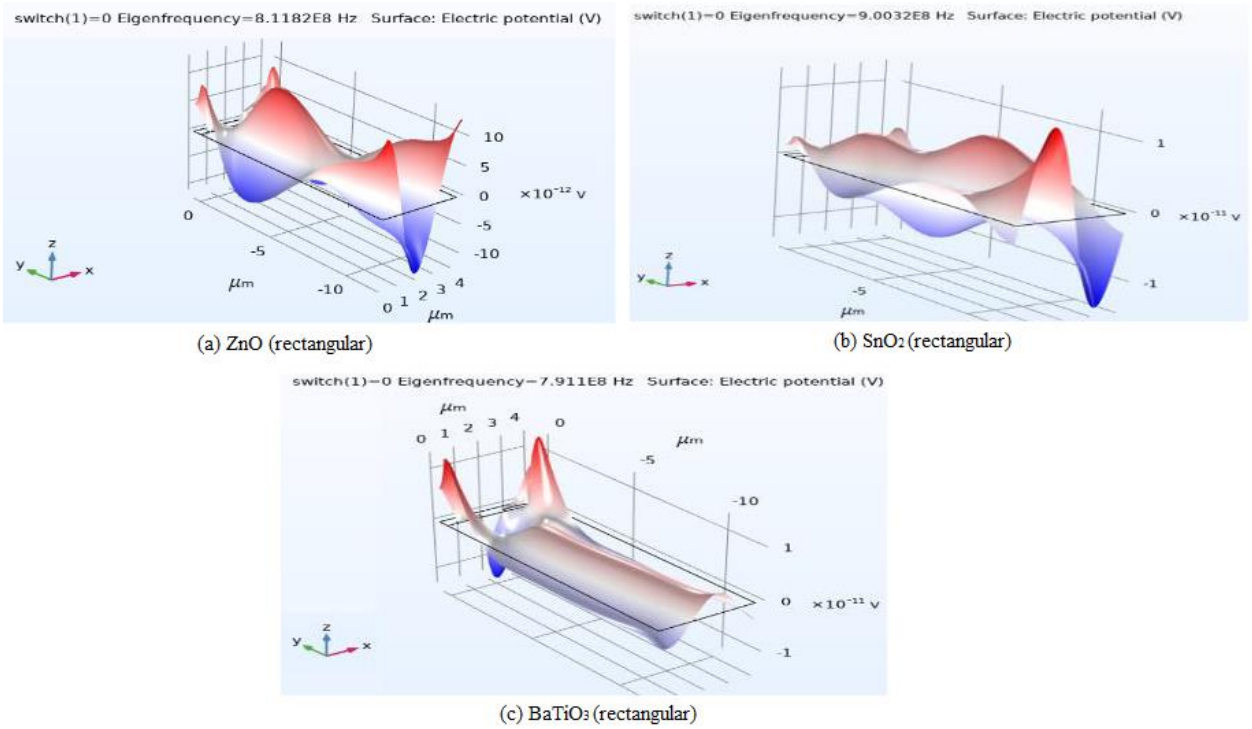

(a) ZnO (rectangular) (b) SnO_2 (rectangular)

(c) $BaTiO_3$ (rectangular)

Figure 7 Electric potential (V) of the rectangular architecture of the saw gas sensor

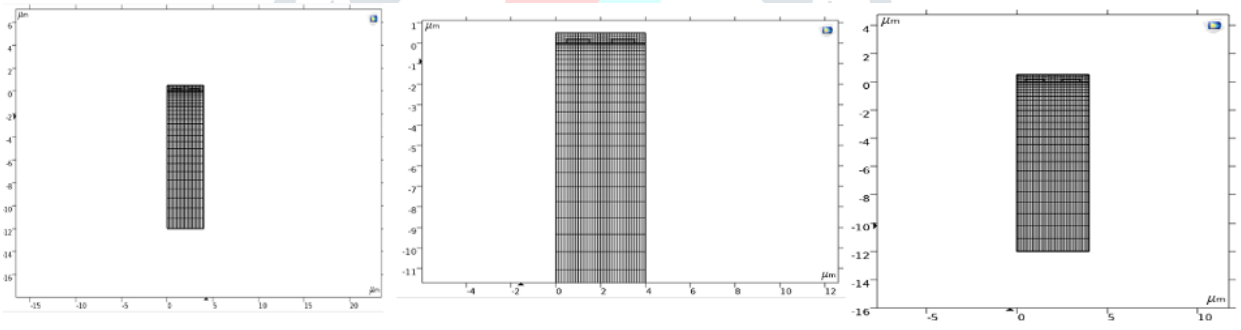

Figure 8 Meshed designed model with two electrodes

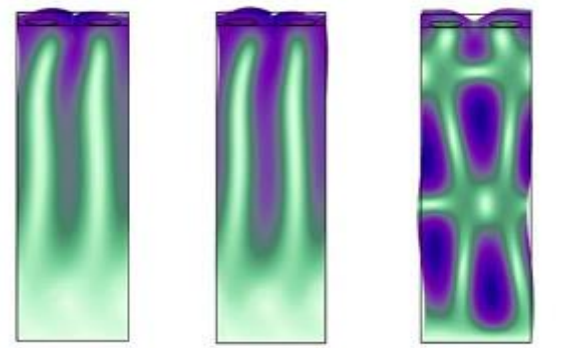

(d) Zinc Oxide (e) Tin Oxide (ellipse) (f) Barium Titanate (ellipse)

Figure 9 Elliptical structure for IDTs

Consequently, the width ranged from 0.2 μm to 1.2 μm and the output potential that is attained at an interval of 0.2 is recorded. The outcomes of each simulation are recorded for both structures and plots are used.

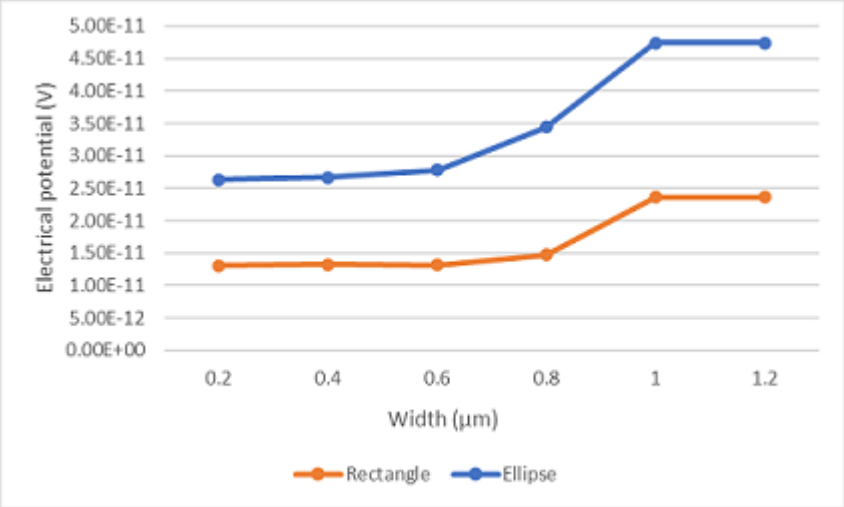

Figure 10 For rectangular and elliptical structures, width versus electric potential

Figure 10 show that the elliptical structure outperforms the rectangular structure in terms of output. Elliptical structures take up less space than rectangular structures of the exactly same width. Because the output is consistent throughout the range of 0.6 μm to 1.2 μm, 1 μm is chosen as the IDT structure's best width. Figure 11 shows the displacement of the surface (μm) of the elliptically constructed SAW gas sensor to the chosen substrate material. The displacement of the surface is one of the outputs achieved with varied eigenfrequency input values.

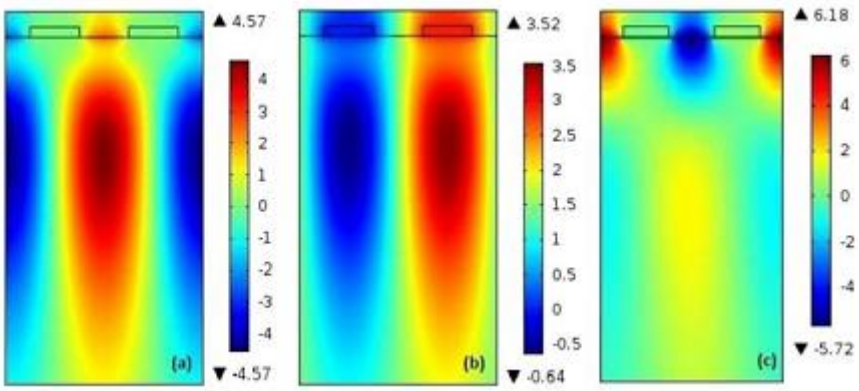

Figure 11 the displacement of the Surface (μm) of the saw gas's circular architecture

Figure 12 illustrates the electric potential (V) produced by an elliptical structure SAW sensor. For various input eigen frequency values, the output electric potential fluctuates. An electric potential is shown with its highest value in the red colour zone, fading to blue for lesser values. Figure 13 illustrates the comparison graph of rectangular and elliptical structures for the three materials. Based on the findings of the investigation, the displacement of the surface of designing an elliptical structure seems to be bigger and greater than the rectangular structure.

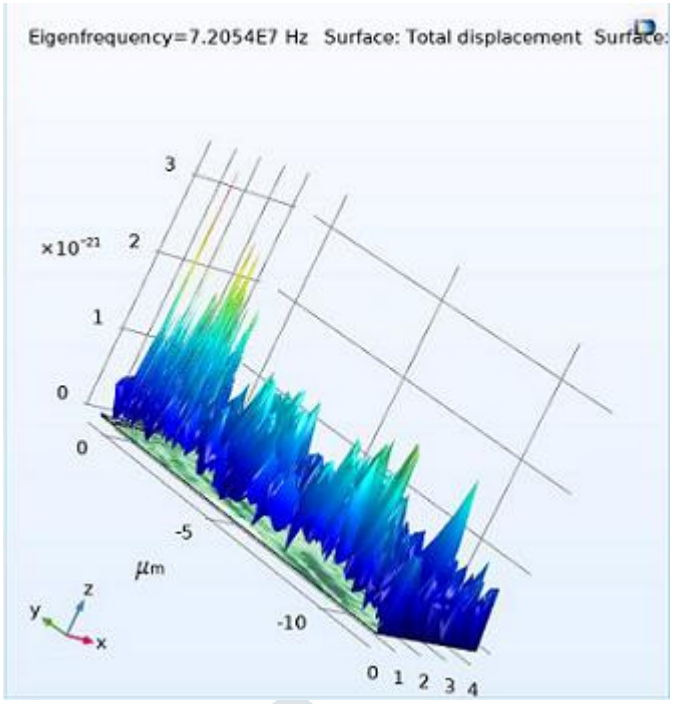

Figure 12 The electrical potential (V) of saw gas sensor elliptical construction

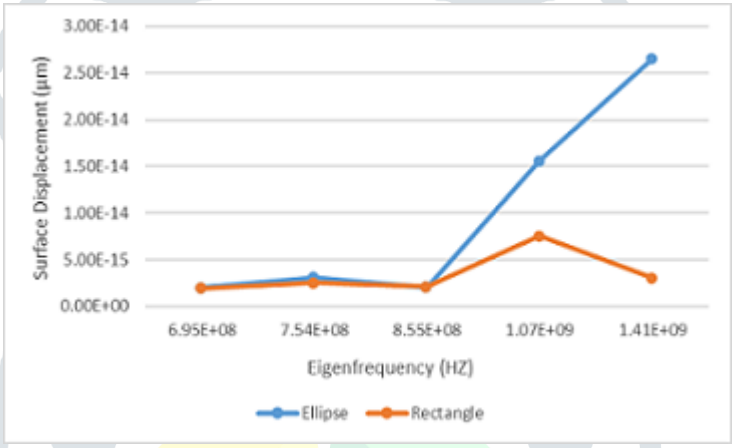

Figure 13 Eigen frequency vs surface displacement for rectangular and elliptical

Figure 14 demonstrates how the electric potential varies with eigenfrequency for rectangle and elliptic shapes. According to the analysis of the graph, the O/P value, the ellipse has a large electric potential. Since elliptical structures have greater displacement of the surface and electric potential than rectangular structures, they can be used to design SAW sensors. Three piezoelectric materials were compared for separate rectangle and elliptical forms is part of the investigation of materials. The substrate's substance was chosen to be ZnO, SnO_2, and $BaTiO_3$. Figure 15 shows the eigen frequencies versus the displacement of the surface for three distinct piezoelectric materials of the rectangle structure. The graph clearly shows that the displacement of the surface for $BaTiO_3$ is larger than for the other minerals studied. $BaTiO_3$ has optimum characteristics for the material used in the gas sensor because it provides a higher output (the displacement of the surface).

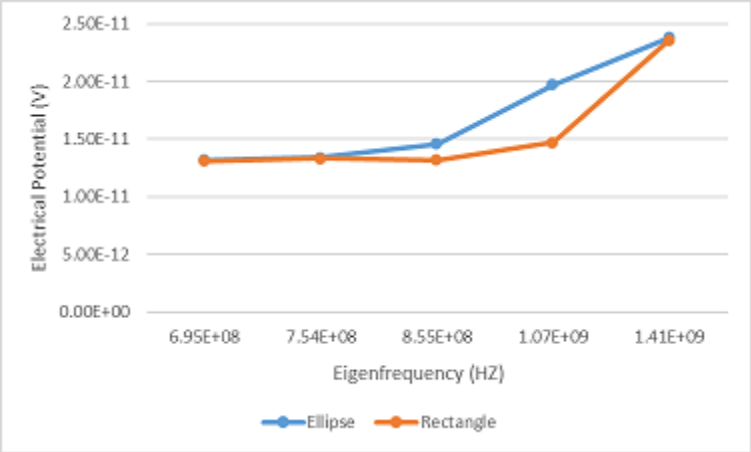

Figure 14 Eigen frequency as a function of electric potential for rectangular and elliptical structures

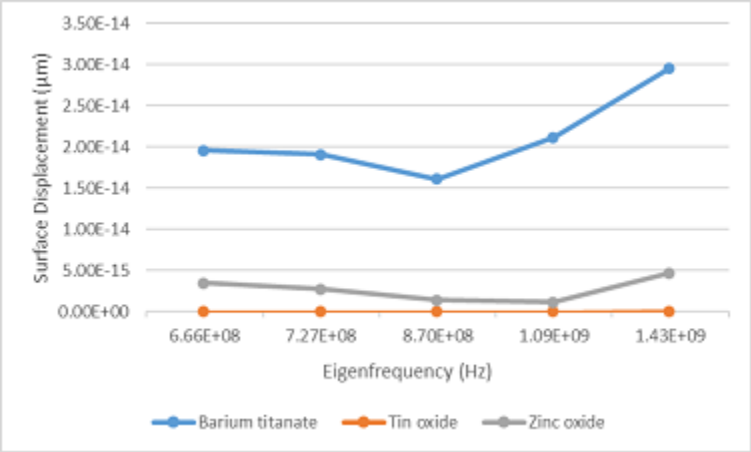

Figure 15 Electric potential versus the displacement of the surface for various materials

For various piezoelectric materials used in rectangular structures, Figure 16 displays the electric potential versus surface displacement.

In the graph, the materials with higher electric potential include ZnO, SnO_2, and $BaTiO_3$. Compared to other materials, $BaTiO_3$ exhibits an almost steady electric potential. Since $BaTiO_3$ has higher outputs (the displacement of the surface and electric potential), it may be employed as the substrate material to boost its sensitivity.

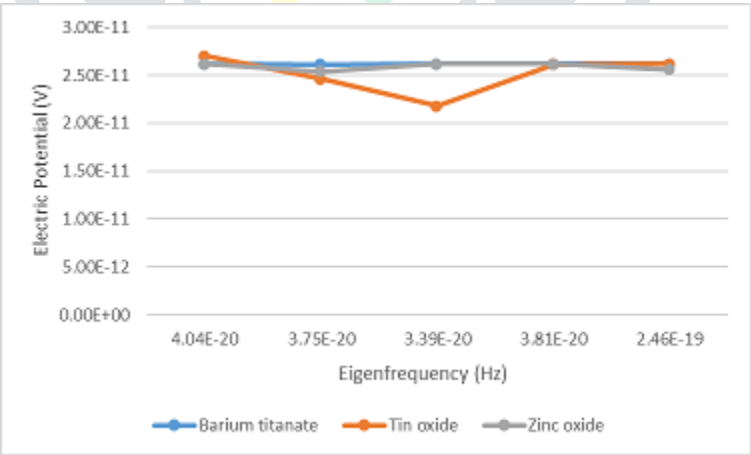

Figure 16 Electric potential versus the displacement of the surface for various materials

Figure 17 shows eigen frequencies versus the displacement of the surface for the elliptical structure's three distinct piezoelectric substances. The graph clearly shows that $BaTiO_3$ has a higher surface displacement than other

materials. $BaTiO_3$ produces a higher output in surface displacement, so it may be employed as the substrate material in the gas sensor.

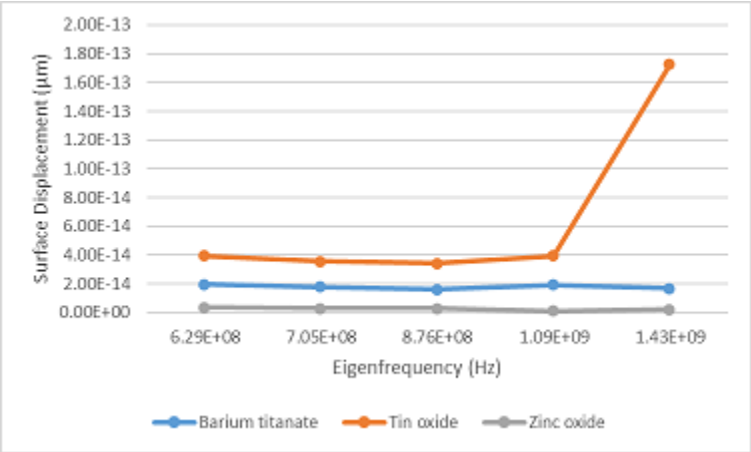

Figure 17 Eigen frequency versus the displacement of the surface for elliptical

Figure 18 depicts the electric potential against the displacement of the surface for various elliptical piezoelectric substances. The graph shows, ZnO and $BaTiO_3$have similar electric potentials. Because BaTiO3 has higher outputs (the displacement of the surface and electric potential), it is a suitable material to use as a substrate to increase its sensitivity.

According to the comparative study among the different materials where are used (ZnO, SnO_2, and $BaTiO_3$), $BaTiO_3$ has shown better output values of the power consumption which is 30 mW, high sensitivity which is 49, and a high velocity is 5700 m/s. Table 2 summarizes all the previous results from figures (10-18) with the comparison using different materials (ZnO, SnO_2, and $BaTiO_3$).

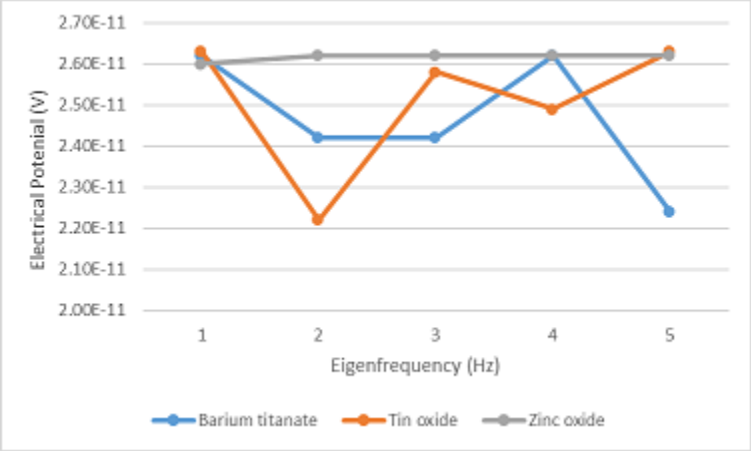

Figure 18 Eigen frequency versus electric potential for elliptical

Conclusion

In this paper, The MEMS gas sensor is based on surface acoustic waves (SAW) which features benefits such as compact size, cheap manufacturing cost, extended lifespan, high level of sensitivity and selectivity. The SAW gas sensor is mainly used in chemical industries, military applications, and used in wireless sensing applications. A comparative study between two different designs for SAW gas sensors that differ in the shape of IDTS is designed and simulated using COMSOL Multiphysics 5.5.

The SAW gas sensor construction initially is composed of three major regions which is a rectangle piezoelectric substrate, a rectangle sensing layer, and interdigitated transducers (IDT) again for two different forms rectangular and elliptical.

Three piezoelectric materials (ZnO, SnO_2, and $BaTiO_3$) are compared in terms of the displacement of the surface, the potential of electric, the frequency of eigenvalues, sensitivity, Power consumption, and velocity while fixing the values of temperature (293K). It has been observed that the interdigitated transducer of the SAW gas sensor's ellipse-shaped construction using $BaTiO_3$ material introduced the device's optimum performance in terms of sensitivity (49), velocity (5700 m/s), and power consumption (30 mW) as shown in Table 2 than the other materials.

Table 2 displays a comparative study of the two designs and the three piezoelectric materials

Shape	**Rectangular**			**Enhanced Ellipse**		
Material	***Zinc oxide***	***Tin oxide***	***Barium Titanate***	***Zinc oxide***	***Tin oxide***	***Barium Titanate***
Eigen frequency (Hz)	66.64E+07 72.76E+07 81.58E+07 10.92E+08 14.34E+08	62.92E+07 70.43E+07 81.58E+07 10.911E+08 14.351E+08	71.71E+07 72.25E+07 81.58E+07 10.23E+08 14.31E+08	66.701E+07 72.701E+07 81.58E+07 10.92E+08 14.23E+08	62.90E+07 70.51E+07 81.58E+07 10.91E+08 14.32E+08	71.71E+07 71.81E+07 81.58E+07 10.23E+08 14.32E+08
Surface Displacement (μm)	35.11E-16 27.43E-16 13.91E-16 11.92E-16 47.15E-16	40.42E-21 37.52E-21 33.94E-21 38.12E-21 24.62E-20	19.65E-15 19.10E-15 16.11E-15 21.23E-15 29.65E-15	34.51E-16 28.41E-16 13.93E-16 12.41E-16 21.91E-16	39.41E-15 35.53E-15 34.31E-15 39.61E-15 17.34E-14	19.64E-15 17.92E-15 16.01E-15 19.22E-15 16.91E-15
Electric Potential(V)	26.28E-12 25.45E-12 26.23E-12 26.27E-12 25.63E-12	27.01E-12 24.06E-12 21.82E-12 26.11E-12 26.12E-12	26.23E-12 26.21E-12 26.23E-12 26.23E-12 26.23E-12	26.0E-12 26.2E-12 26.2E-12 26.2E-12 26.2E-12	26.31E-12 22.25E-12 25.84E-12 24.92E-12 26.31E-12	26.23E-12 24.25E-12 26.23E-12 26.23E-12 22.41E-12
Temperature	293 (K)	293 (K)	293 (K)	293 (K)	293 (K)	293 (K)
Velocity	2655 m/s	3750 m/s	5700 m/s	2655 m/s	3750 m/s	5700 m/s
Sensitivity	29.7	32	43	32	40	49
Power	44 mW (< 1OO	37 mW (< 1OO	35 mW (< 1OO	40 mW (< 1OO mW)	34 mW (< 1OO	30 mW (< 1OO

consumption	mW)	mW)	mW)		mW)	mW)
Dimension	Sensor width: width Sensor height: 3*width+t_PIB IDT width: width/4 IDT height: 0.4*t_PIB			Sensor width: width Sensor height: 3*width+t_PIB IDT a-semiaxis: 0.6 IDT b-semiaxis: 0.11		

References

[1] Attallah, O., & Morsi, I. (2022). An Electronic Nose For Identifying Multiple Combustible/Harmful Gases And Their Concentration Levels Via Artificial Intelligence. Measurement, 199, 111458.

[2] Morsi, I. (2010). Electronic Nose System And Artificial Intelligent Techniques For Gases Identification. Data Storage.

[3] Shokry Hassan, H., Kashyout, A. B., Morsi, I., Nasser, A. A. A., & Ali, I. (2014). Synthesis, Characterization And Fabrication Of Gas Sensor Devices Using Zno And Zno:In Nanomaterials. Beni-Suef University Journal Of Basic And Applied Sciences, 3(3), 216–221.

[4] He, L. X., Wang, F., Niu, G. Q., Gong, H. M., Yang, Z. T., He, W., & Cao, J. M. (2018). Design Of MEMS-Based Gas Sensor Micro Heat Plate. Proceedings Of The International Workshop On Materials, Chemistry And Engineering.

[5] Teja, N. V., Harathi, N., Sarkar, A., & Priya, K. S. (2019). Modeling Of MEMS-Based Surface Acoustic Wave-Gas Sensor To Obtain Enhanced Sensitivity. 2019 3rd International Conference On Electronics, Materials Engineering & Nano-Technology (Iementech).

[6] Mazalan, M., Noor, A., Wahab, Y., Yahud, S., & Zaman, W. (2021). Current Development In Interdigital Transducer (IDT) Surface Acoustic Wave Devices For Live Cell In Vitro Studies: A Review. Micromachines, 13(1), 30.

[7] Zhou, J., Shi, X., Xiao, D., Wu, X., Zheng, J., Luo, J., Zhuo, M., Tao, X., Jin, H., Dong, S., Tao, R., Duan, H., & Fu, Y. Q. (2018). Surface Acoustic Wave Devices With Graphene Interdigitated Transducers. Journal Of Micromechanics And Microengineering, 29(1), 015006.

[8] Zhou, Z., Tan, J., Zhang, J., &Amp; Qin, M. (2019). Structural Optimization And Analysis Of Surface Acoustic Wave Biosensor Based On Numerical Method. International Journal Of Distributed Sensor Networks, 15(9), 155014771987564.

[9] Morsi, I., &Amp; Kashyout, A. B. (2016, July). Fabrication Of High Sensitive Zno Gas Sensor For LPG Gas Detection. Research Gate. Retrieved April 2, 2023, From https://www.Researchgate.Net/Publication/364456426.

[10] Ibrahim, Y., Kashyout, A. B., Morsi, I., & Shokry Hassan, H. (2020). Development Of Nano-SnO2 And SnO2:V2O5 Thin Films For Selective Gas Sensor Devices. Arabian Journal For Science And Engineering, 46(1), 669–686.

[11] Shi, D., Guo, Z., & Bedford, N. (2015). Electro-Optical and Piezoelectric Applications Of Zinc Oxide. Nanomaterials and Devices, 175–190.

[12] Wang, S.-Y., Ma, J.-Y., Li, Z.-J., Su, H. Q., Alkurd, N. R., Zhou, W.-L., Wang, L., Du, B., Tang, Y.-L., Ao, D.-Y., Zhang, S.-C., Yu, Q. K., &Amp; Zu, X.-T. (2015). Surface Acoustic Wave Ammonia Sensor Based On ZnO/SiO2 Composite Film. Journal Of Hazardous Materials, 285, 368–374.

[13] Chen, J., Guo, H., He, X., Wang, W., Xuan, W., Jin, H., Dong, S., Wang, X., Xu, Y., Lin, S., Garner, S., & Luo, J. (2015). Development of flexible ZnO thin film surface acoustic wave strain sensors on ultrathin glass substrates. Journal of Micromechanics and Microengineering, 25(11), 115005.

[14] Abdelghani, R., Shokry Hassan, H., Morsi, I., &Amp; Kashyout, A. B. (2019). Nano-Architecture Of Highly Sensitive SnO2–Based Gas Sensors For Acetone And Ammonia Using Molecular Imprinting Technique. Sensors And Actuators B: Chemical, 297, 126668. Https://Doi.Org/10.1016/J.Snb.2019.126668

[15] S.Ibrahim, Sh Ebrahim I. Morsi. (2011). Pyroelectric Properties Of Nanocomposite Of Polyvinylidene Fluoride And BaTiO3. International Conference On Mechanical Engineering And Technology (ICMET-London 2011), 311–315.

[16] S, M. A., S D, B. S., & R, S. P. (2021). Optimizing Design Of Surface Acoustic Wave Gas Sensor. 2021 5th International Conference On Trends In Electronics And Informatics (ICOEI).

[17] Li, C., Liu, X., Shu, L., &Amp; Li, Y. (2015). ALN-Based Surface Acoustic Wave Resonators For Temperature Sensing Applications. Materials Express, 5(4), 367–370.

[18] Tang, Y., Li, Z., Ma, J., Wang, L., Yang, J., Du, B., Yu, Q., &Amp; Zu, X. (2015). Highly Sensitive Surface Acoustic Wave (SAW) Humidity Sensors Based On Sol–Gel SiO2 Films: Investigations On The Sensing Property And Mechanism. Sensors And Actuators B: Chemical, 215, 283–291.

[19] Morsi, I., Zaghloul, M. S., &Amp; Essam, N. (2010). Future Voyage Data Recorder Based On Multi-Sensors And Human Machine Interface For Marine Accident. ICCAS 2010.

[20] Oppenheim, I.J., P. Z. D. W. G. (2009). Multiphysics Simulation Of The Effect Of Sensing And Spacer Layers On SAW Velocity. In COMSOL Conference,Boston..

[21] Lucia, F. D., Jr, P. Z., Frazatto, F., Piazzetta, M., &Amp; Gobbi, A. (2014). Design, Fabrication And Characterization Of SAW Pressure Sensors For Extreme Operation Conditions. Procedia Engineering, 87, 540–543.

[22] Salim, Z.T., Hashim, U., Arshad, M.K., & Fakhri, M.A. (2016). Simulation , Fabrication And Validation Of Surface Acoustic Wave Layered Sensor Based On ZnO / IDT / 128 ° YX LiNbO3.

[23] Liu, B., Chen, X., Cai, H., Mohammad Ali, M., Tian, X., Tao, L., Yang, Y., &Amp; Ren, T. (2016). Surface Acoustic Wave Devices For Sensor Applications. Journal Of Semiconductors, 37(2), 021001.

[24] Ramakrishnan, N., Namdeo, A. K., Nemade, H. B., &Amp; Palathinkal, R. P. (2012). Simplified Model For FEM Simulation Of SAW Delay Line Sensor. Procedia Engineering, 41, 1022–1027.

[25] Sil, D., Hines, J., Udeoyo, U., &Amp; Borguet, E. (2015). Palladium Nanoparticle-Based Surface Acoustic Wave Hydrogen Sensor. ACS Applied Materials &Amp; Interfaces, 7(10), 5709–5714.

[26] Kutiš, V., Gálik, G., Královič, V., Rýger, I., Mojto, E., &Amp; Lalinský, T. (2012). Modelling And Simulation Of SAW Sensor Using FEM. Procedia Engineering, 48, 332–337.

[27] Zhang, H., &Amp; Wang, H. (2021). Investigation Of Surface Acoustic Wave Propagation Characteristics In New Multilayer Structure: SiO2/IDT/LiNbO3/Diamond/Si. Micromachines, 12(11), 1286.

[28] Sun, X., Liu, W., Shao, X., Zhou, S., Wang, W., &Amp; Lin, D. (2018). Surface Acoustic Wave Gyroscopic Effect In An Interdigital Transducer. Sensors, 19(1), 106.

[29] W., R. C. C., &Amp; Fjeldly, T. A. (2001). In Advances In Surface Acoustic Wave Technology, Systems And Applications. Singapore; World Scientific.

[30] Hikita, M., Minami, K., Takimoto, K., &Amp; Hiraizumi, Y. (2008). Investigation Of Novel Surface Acoustic Wave (SAW) Gas Sensor Used In Sensor Network. PIERS Online, 4(3), 346–350.

[31] Hasan, M. N., Maity, S., Sarkar, A., Bhunia, C. T., Acharjee, D., &Amp; Joseph, A. M. (2016). Simulation And Fabrication Of SAW-Based Gas Sensor With Modified Surface State Of Active Layer And Electrode Orientation For Enhanced H2 Gas Sensing. Journal Of Electronic Materials, 46(2), 679–686.

[32] Hsueh, T.-J., &Amp; Ding, R.-Y. (2022). A Room Temperature ZnO-NPS/MEMS Ammonia Gas Sensor. Nanomaterials, 12(19), 3287.

[33] Scholl, G., Schmidt, F., &Amp; Wolff, U. (2001). Surface Acoustic Wave Devices For Sensor Applications. Physica Status Solidi (A), 185(1), 47–58.

[34] Malik, A. F., Jeoti, V., Fawzy, M., Iqbal, A., Aslam, Z., Pandian, M. S., &Amp; Marigo, E. (2016). Estimation Of Saw Velocity And Coupling Coefficient In Multilayered Piezo-Substrates Aln/SiO2/Si. 2016 6th International Conference On Intelligent And Advanced Systems (ICIAS).

[35] Sreeja, S. D., Gopalan, S., &Amp; Sreekala, C. O. (2019). Piezoelectric Energy Harvesting System Suitable For Remotely Placed Sensors With Inter-Digitated Design. Proceedings Of The International Conference On Advanced Materials: Icam 2019.

[36] Maramizonouz, S., Jia, C., Rahmati, M., Zheng, T., Liu, Q., Torun, H., Wu, Q., &Amp; Fu, Y. Q. (2022). ACOUSTOFLUIDIC Patterning Inside Capillary Tubes Using Standing Surface Acoustic Waves. International Journal Of Mechanical Sciences, 214, 106893.

[37] Floer, C., Hage-Ali, S., Nicolay, P., Chambon, H., Zhgoon, S., Shvetsov, A., Streque, J., M'Jahed, H., &Amp; Elmazria, O. (2020). Saw RFID Devices Using Connected Idts As An Alternative To Conventional Reflectors For Harsh Environments. IEEE Transactions On Ultrasonics, Ferroelectrics, And Frequency Control, 67(6), 1267–1274.

[38] Mishra, D., &Amp; Singh, A. (2015). Sensitivity Of A Surface Acoustic Wave Based Gas Sensor: Design And Simulation. 2015 International Conference On Soft Computing Techniques And Implementations (ICSCTI).

[39] Patial, P. (2021). Design And Development Of Efficient Semiconductor-Based Surface Acoustic Wave Gas Sensor: A Systematic Review. The Era Of Nanotechnology, 245–255.

[40] Mishra, D. (2015). Modeling Of Interdigital Transducer Surface Acoustic Wave Device - Design And Simulation. 2015 Fifth International Conference On Communication Systems And Network Technologies.

[41] Mujahid, A., &Amp; Dickert, F. (2017). Surface Acoustic Wave (SAW) For Chemical Sensing Applications Of Recognition Layers. Sensors, 17(12), 2716.

[42] Kelly, L. (2022). Fabrication And Characterization Of 2-Port Surface Acoustic Wave (Saw) Resonators For Strain Sensing (Thesis). Faculty Of Science University Of Ottawa, Canada.

[43] Kandel, Y. P. (N.D.). Surface Acoustic Wave Resonator. Surface Acoustic Wave Resonator. Retrieved March 22, 2023, From http://www2.optics.rochester.edu/workgroups/cml/opt307.